Damage Evolution on Different Scales

L.R. Botvina

Institute of Metallurgy and Materials Science, Russian Academy of Sciences, 49 Leninskij prospect, 199911 Moscow, Russia

botvina@ultra.imet.ac.ru

Keywords: plastic zone, acoustic emission, cumulative distribution of microcracks, amplitude distribution of acoustic signals, fracture magnitude, fragmentation

Abstract. The patterns of multiple fractures in carbon steel specimens at different stages of tension, cyclic and dynamic loading were studied; characteristics of damage accumulation were estimated and the cumulative number-length distributions of microcracks were plotted. The parameters of these distributions were compared with those of both the amplitude distributions of acoustic emission signals during tension and the magnitude distributions of seismic events, which accompany the formation of multiple faults in the earth crust before earthquake. The study allowed us to found the similarity of the kinetic features of the damage evolution on different scales, to establish general laws of damage accumulation, and to suggest a physical interpretation of the parameters proposed for the earthquake prediction.

Introduction

Many examples of the similarity of the multiple fracture patterns observed on the micro-, macro- and global level of the development of kinetic processes testify about the unity of nature and possibility to use small specimens for modeling the kinetics of tectonic processes on the basis of the approaches of the solid mechanics and physics of fracture. The founder of tectonophysics M.V.Gzovskiy [1] has supposed that for such modeling, along with the above-mentioned approaches, it is necessary to ensure both geometric and physical similarity. However it is not always possible to fulfill this condition; therefore, another approach based on the similarity of the basic kinetic regularities was used. Such a similarity of the fracture kinetic processes on different scale levels will be discussed below.

Localized zones of deformation and fracture

Damage evolution on any scale level begins with a localization of deformation or fracture near structural or mechanical stress concentrators. Information about the strain localization process can be obtained using the method of replicas of the lateral surface of specimens taken at different loading stages.

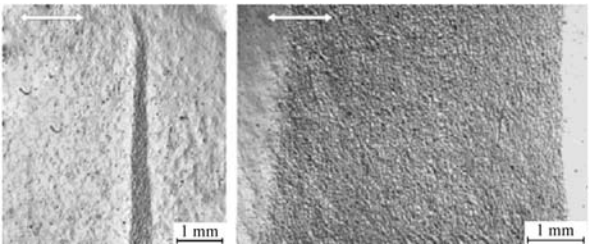

Fig. 1. Change in area of a plastic zone on the lateral side of low-carbon steel specimen under cyclic tension with increasing a number of cycles (the loading direction is shown by arrows).

Under tension (or cyclic loading) of *smooth specimens* performed from a *ductile material*, the localization of deformation is related to the formation of the Lüders bands, their passage along a specimen and increase in the band width, which leads to the development of the continuous deformed region. The crack initiates inside the deformation zone (Fig. 1), and structural and mechanical concentrators facilitate this process.

Localization of deformation in the smooth specimens made of the same steel that is in *a quasi-brittle* state resulting from the natural aging, is also connected with the passage of Lüders's macrobands. However in this case, the density of these bands is lower than that in the ductile material; the continuous plastic zone is not formed, and no slip inside grains almost is observed. This leads to the formation of microcracks at the initial stage of deformation and their elongation. Similar microcracks are also found in brittle and quasi-brittle rocks.

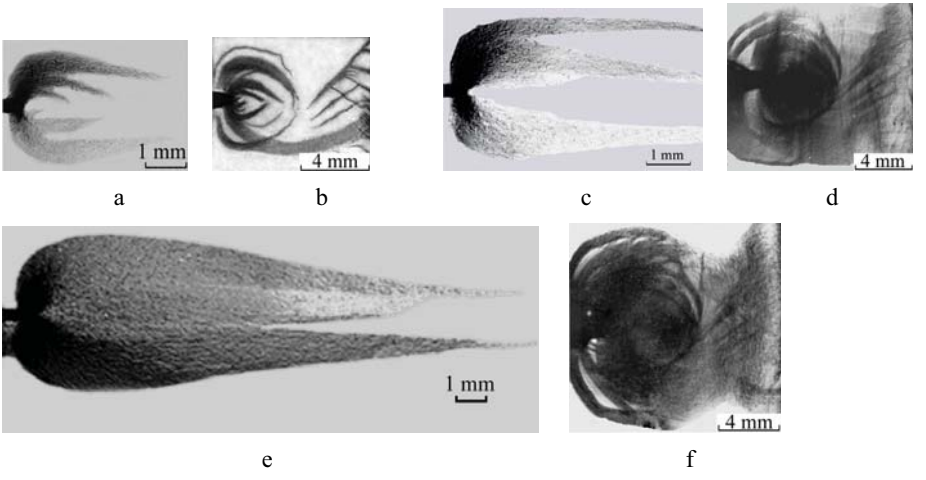

Fig 2. Plastic zones at the notch tip of low-carbon steel specimens (a, c, e) 2.5 and (b, d, f) 16 mm thick at different loading stages under relative loads P/P_{max} of (a, b) 0.6, (c, d) 0.8 and (e, f) 0.9.

At testing *a notched specimen,* the localized zone is formed near the notch tip. As the specimen thickness increases, a radius of plastic zone under tension is known, to reduce. This leads to a change in the local stress state of material, that is accompanied by a reduction in fracture toughness and a change in the shape of plastic zone (Fig. 2).

A similar change in the shape of plastic zone was revealed also *on the microlevel,* i.e. in studying the zone of strain localization at the tips of sulfide inclusions with the length of 0.5 mm by microhardness measurement. The specimens from low alloyed steel were hydrogen charged at a tensile load with different holding periods in this corrosion medium. The microhardness measurements in several directions in relation to the sulfide axis showed that a holding in the corrosive medium leads to a decrease in the plastic zone and change in its shape that is similar to that in the shape of the macro-zones of plastic deformation in the range of transition from the plane stress to the plane strain state (see Fig. 2). The results have shown also that two plastic zones with different hardening degree appeared at the inclusion tips similar to the formation of two plastic zones at the main crack tip under tension.

The picture of strain localization *at cyclic loading* of notched specimen from the same steel depends on the stress amplitude, namely, a number of microcracks are formed at the low stress amplitudes, whereas cascade of expanding plastic zones appears at the high amplitudes (Fig. 3). This fatigue fracture mechanism at the low stress amplitudes seems to be similar to mechanism of the slip-strike growth of cracks in rocks (see the left top micrograph in Fig.3).

The *dynamic loading* of shells at a rate exceeding of 1000 m/s leads to a multiple fracture with the formation of numerous shear and rupture microcracks surrounded by a zone of pores.

Thus, the shape of the localized zones is determined by loading conditions, properties of material, and geometry of specimen or inclusion. With increasing load before a critical event (specimen fracture), the size of zones or the number of multiple fracture origins grows. This is demonstrated also by data on the acoustic emission measured during experiment [2]: in testing the specimen, the correlation radius of acoustic activity grows and corresponds to the radius (or length) of plastic zone, which exceeds the length of the microcracks formed in the zone by 1-3 orders of magnitude.

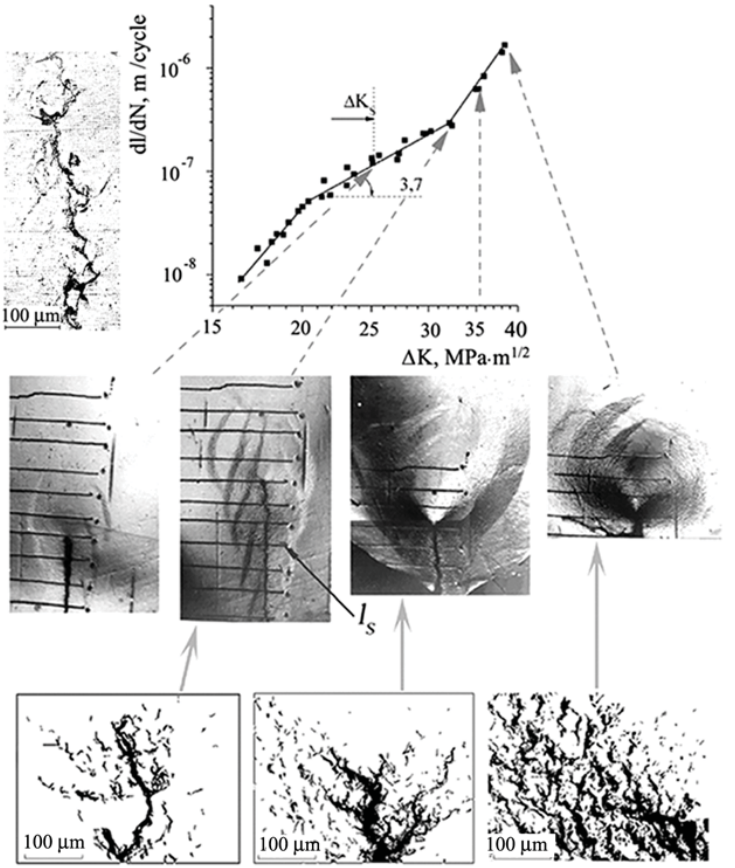

Fig. 3. Kinetic diagram of the fatigue fracture of low-carbon steel and plastic deformation zones at different stages of a crack growth. (The distance between marks on the specimen surface is equal to 1 mm; the loading direction is perpendicular to the crack growth one. The left top micrograph shows a trajectory of the main crack at $\Delta K \approx 22$ MPa$\sqrt{m}$).

The same process occurs also on *the global level* during the development of faults of the rocks. The approach a critical event (the earthquake), which is accompanied by the appearance of faults leads to an increase in the seismic activity area characterized also by the correlation radius.

The measurement of both the length (R_y) of the plastic zone accepted for a correlation radius of the damage accumulation process, and corresponding energy of fracture (E) at different loading stages that was evaluated from the area under deformation curve allowed us to plot the dependence of R_y on the fracture magnitude M^* for low carbon steel specimens [3]. The fracture magnitude was calculated [4] by the relationship utilized in seismology: $1.5M = \log E - 4.8$ (J). The results of these estimations showed that the fracture localization zone in the laboratory specimens differening in thickness was proportional to the fracture magnitude $\log R_y \sim 0.94\ M^*$. The dependence obtained is found to be similar to that characterizing a change in the correlation radius R_C of seismic activity in different regions of the world, which is proportional to the magnitude M of the earthquake: $\log R_C \sim$ of $0.44\ M$ [5, 6].

Structure of fracture localized zones

Let us examine now *the structural level* of the response of material on the applied load that is characterized by defects from 5 to 500 μm in size, i.e., differing from the localized zone sizes by 2-3 orders of magnitude.

The beginning of *tensile deformation* of a specimen made of a ductile material is accompanied by the appearance of chains of pores along the grain boundaries located near the notch tip (Fig. 4, a). Then slip bands inside the grains are developed, and the deformation zone is formed. The pores are accumulated in the slip bands and microcracks appear as a result of their coalescence.

Under *cyclic loading* of *smooth specimen*, deformation of grains is considerably smaller, but the fracture sequence remains the same: first, the deformation is located at grain boundaries, at which pores appear subsequently. With increasing load, transgranular slip is developed, clusters of the slip bands, chains of pores in the bands and in mechanical stress concentrators (scratches) appear (Fig. 4 b). With increasing deformation, the density of slip bands grows, the clusters of slip bands appear, the pores are formed inside the bands, the distance between the pores in the chain approaches a diameter of pore itself; after that pores merge and microcracks, the majority of which has a size close to an average grain diameter, are formed.

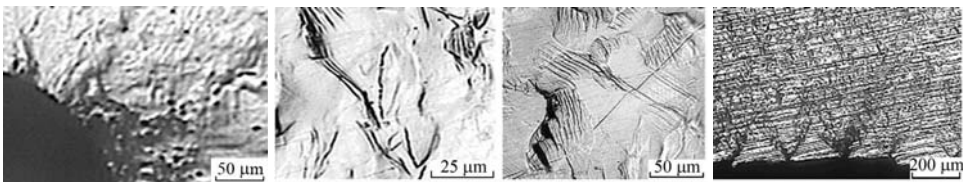

a b c d

Fig. 4. Structure of plastic zone (e) in notched low-carbon steel specimens tested at tension and in (b-d) smooth specimens from the same steel tested under cyclic loading

Then chains or clusters of the defects of the next hierarchical level (microcracks) appear, length and opening of these defects grow (Fig. 4 c, d). The process of the damage development is accompanied by shear along the grain boundaries that manifests itself in the displacement of the scratch line of (Fig. 4, c). In parallel with the process of the damage accumulation in the central zones of specimen, numerous microcracks are developed from defects on the lateral specimen side, one of which becomes the origin of the fatigue main crack. In quasibrittle materials no macrozone of plastic deformation is formed, and microcracks appear at the initial stage of deformation.

Under *dynamic loading*, numerous shear microcracks (Fig. 5, a) and the bands of adiabatic shear (Fig. 5, b, c) with the pores are observed. The coalescence of the pores leads to the formation of new shear cracks. Near the cracks, the region of multiple damage (Fig.5, b) accompanying the shear crack development is revealed.

Thus, for all types of loading, the damage development at different hierarchical levels is related to the formation of chains of defects, during the coalescence of which a defect of the next level appears.

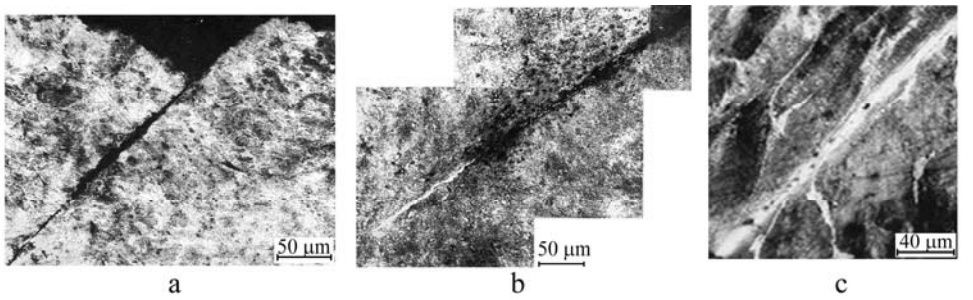

Fig. 5. Structure of fracture localized zones at dynamic loading

As is followed from many studies on seismology, the formation of faults in the earth crust is also caused by appearance of chains of small faults whose coalescence leads to the appearance of longer faults accompanied by earthquake of large magnitude. The forming of the chains of small faults must to be reflected in the appearance of chains of seismic events. Indeed, the algorithm of the earthquake prediction proposed recently and approved in practice [7] is based on the revealing and registration of such chains, which are the precursors of large earthquakes.

Cumulative number-length distributions of microcracks and amplitude distributions of acoustic emission signals

The use of replicas gives the possibility not only to measure the plastic zones and to study their structure, but also to plot the number - length distributions of microcracks at different loading stages. The maximum number of microcracks measured for each specimen was 1500-10000; it depended on the material damage at the studied loading stage. The results of measurements were used for plotting the cumulative number-length distributions of microcracks, i.e., the distributions of the total number (N) of microcracks with the length (l) equal or more than each measured length. In plotting the distributions, the microcrack length changes by 1.5 - 2 orders of magnitude.

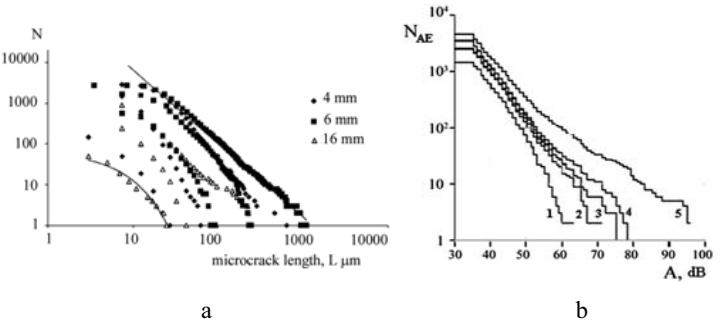

Fig. 6. (a) Cumulative number – length distributions of microcracks at tension of low-carbon steel specimens and (b) amplitude distributions of acoustic emission signals received during loading

It was found that, at the initial stages of *tension of the notched specimens*, the distributions of microcracks are described by simple exponential function:
$\lg N_C = A - exp(-cl)$, which changes to the power relation: $\lg N_C = B - b_C \lg l_C$ as a result of both coalescence of microcracks during damage development and increase in the number of long cracks

(Fig. 6, a). The change of the cumulative microcrack distributions manifests itself in similar change of relations describing the amplitude distributions of the acoustic emission signals. In the beginning of loading (Fig. 6, b curve 1), these distributions were described by exponential function

$\lg N_{AE} = D - exp(-c_{AE} l)$, which changes to power function: $\lg N_{AE} = B - b_{AE} \lg l_{AE}$.

The form of cumulative curves at the *cyclic loading of smooth specimens* from the steel investigated obeys the exponential dependence, although it depends on the degree of the material embrittlement. As it follows from Fig.7a, the natural aging of steel results in an increasing the maximum microcrack length and a reduction in their number [8]. In testing *the notched specimens* made of steel in the ductile state, the change of the functions describing the distributions of microcracks was found to be similar to the change of relations revealed at tension (Fig. 7, b).

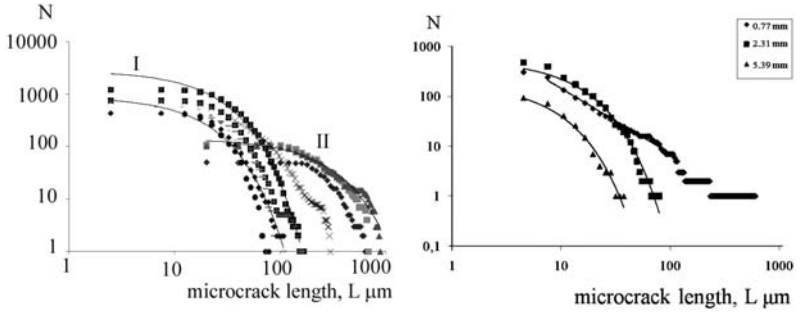

Fig. 7. (a) Cumulative number – length distributions of fatigue microcracks in low-carbon steel specimens: (I) the steel in the initial state and (II) after the natural aging (b) the distribution of microcracks in the notched specimen at different distances from the fracture surface.

The analysis of the distribution curves of microcracks and acoustic emission signals showed that the damage development leads to a reduction in the exponents of the functions describing these distributions. The same conclusion was made, also, based on the data of the amplitude distributions of the acoustic emission signals at tension of DCB-specimen after holding in a corrosion medium [9]. In this case we observed the reduction in the b_{AE} - exponent before the jump of brittle crack related to a drop in the load. This shows that the reduction in the *b*-exponents can be a consequence of the fracture mechanism change.

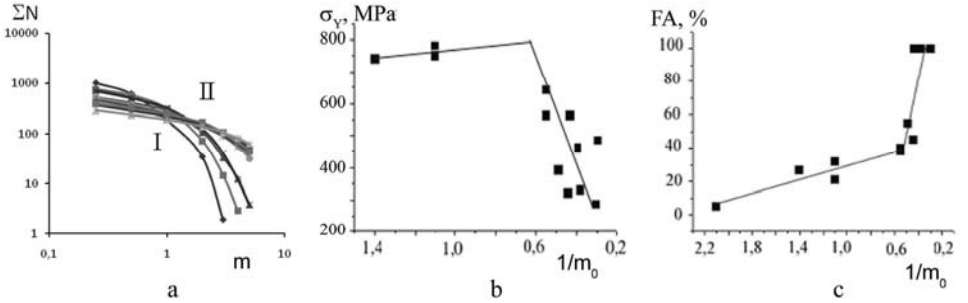

Fig. 8. (a) Cumulative number - mass distributions of fragments (a) formed at the dynamic fracture of shells from steels with different composition and different mechanical properties and (b) the dependences of yield strength and (c) the fibrous area of the fracture surface of the specimens made of material of shells on the characteristic mass (1/mo) of the fragments

The similar conclusion was made, also, in studying the *dynamic fracture* [2] (Fig. 8). The data presented in the Fig. 8 show, firstly, that the number - mass distributions of fragments of shells made of 14 different steels may be described by a simple exponential function:

$\sum N \sim N_O \exp(- m/m_O)$,

and, secondly, that the exponents of these distributions (1/mo) are determined by the mechanical properties of the fragment material (Fig. 8, b, c). As is also seen from Figure 8 a, the curves of the group II, typical of the ductile materials approach the power *N-m* dependences.

In seismology the cumulative dependences of the number of seismic events (N_S) on their energy (E) obey the known power relation of Gutenberg- Richter:

$$\lg N_S = C_S - b_S \lg E = C_S - b_S M$$

Although are there examples of the description of these distributions by simple exponential function [10-12] in the literature. The distributions of the faults in the earth crust also are described by both exponential and power relationships [13].

Stages of the damage accumulation

The estimation of J- integral at tension allows one to connect this parameter of fracture mechanics with the observed stages of accumulation of pores and microcracks (Fig. 10) [14].

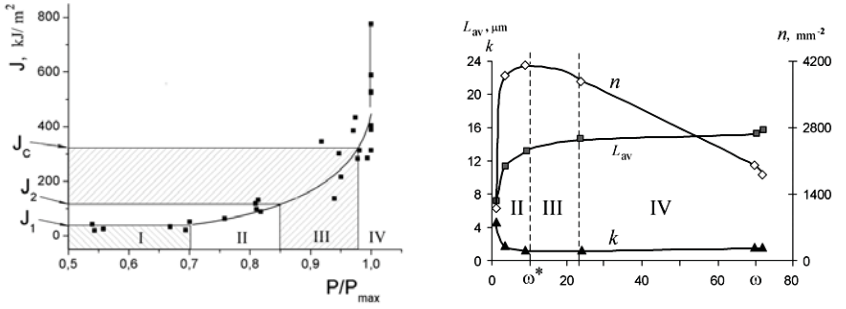

a b

Fig. 9. (a) Dependences of J- integral on the ratio of the current load to the maximum one and (b) the dependences of the average length L_{av}, density of microcracks n and concentration criterion k on the relative fraction of damages ω.

At different stages of tension, the average length of the microcracks L_{av}, their density n, fraction of the damages ω, and the values of concentration criterion k suggested in [15] and estimated by the relation $k = n^{-1/2}/L_{cp}$ were evaluated. Moreover, a fractal dimension of multiple fracture patterns was estimated using the box-counting method [3].

Four stages of the damage accumulation were found. At the first (I) stage, in the notch tip of specimen, slip bands appear and plastic zone is formed (before approaching the yield strength); at the second stage (II), the formation and the accumulation of the microcracks occur. Interaction of microcracks at the third stage (III) leads to their coalescence and initiation of macrocrack as the critical value J_C is reached. At the fourth stage (IV), the main crack appears in a secondary plastic zone in its tip; the area of the damaged surface grows as a result of the opening of microcracks. The development of the main crack leads to the complete fracture. Values J_1 and J_2 characterize the metal resistance to the initiation and accumulation of defects and can be used to control and modify the material structure.

Changes of the damage parameters at the observed stages of multiple fracture are shown in Fig. 9, b. It follows from the graphs that the critical situation appears at reaching the area of damages (ω*) close to 10%, when the microcrack opening increases, density of defects decreases as a result of their coalescence, and concentration criterion falls to the constant value (k~1.5). The value of ω*=10% is close to the threshold of percolation for many systems; therefore, changes at the third stage precede the critical event (specimen fracture). With reaching ω*, the exponential relation, which describes the cumulative distributions of microcracks and acoustic emission signals, becomes close to the power relation, and exponents in these relations reduce. As was shown in [3], the fractal dimension (D_C) of the pattern of microcracks continues to grow, but the rate of the growth is considerably lower as compared to that at the initial stage of the damage accumulation.
The relationship between of the fractal dimension and b_C *–parameter* was found to be linear:
$D_C = 2.86 - 0.67 b_C$. It is similar to the dependence of the correlation fractal dimension D_S on b_S-parameter estimated based on the data of seismic activity:
$D_S = 2,3 - 0.73\ b_S$ [16] and $D_S = 2,72 - 1.39\ b_S$ [17].
As it is noted above, the damage development leads to reduction in the exponents in the relations, which describe the distributions of microcracks. This decrease becomes more substantial in the beginning of coalescence of microcracks, i.e., in transition from stage II to stage III (Fig. 9).

In many studies on seismology, a similar reduction of the exponent b_S in the power equation of Gutenberg - Richter before the strong earthquake and decrease in the concentration criterion, which is used in algorithms of earthquake prediction, are noted [18].

Moreover, in a number of cases, the seismic gap is observed before the strong earthquake. It is connected to the sharp decrease of the number of seismic events and, consequently, also to the decrease in exponent b_S. As was shown in [4], the same acoustic gap is revealed before the fracture of metallic specimen as a result of the initiation of main crack in the notch tip. The period of gap (T_{AE}), is determined by the length of stable crack on the fractures surface of steel specimens. It depends on the strength, ductility of a steel, and radius of notch tip of the specimen (more precise, on the stress state and the stress intensity factor for this material).

The lower the strength and the less the tendency of material to brittle fracture, the greater the period of reduction in the acoustic activity and, therefore, the longer the period of stable growth of crack, which is developed in this case at a low rate. An increase in the radius of specimen notch tip and a reduction in the loading rate lead to the same effect.

Using the new parameter, the fracture magnitude (M*), which is evaluated by the relationship given above, allows us to compare the magnitude dependences of the period of seismic gap (T_S) before the earthquake and acoustic gap (T_{AE}) before the specimen fracture. According to data [19], the period of seismic gap obeys the relation: $\log T_S = 1.2M - 0.9$. The period of acoustic gap observed at the specimen fracture is described by similar relation: $\log T_{AE} = 0.5\ M^* - 0.5$ [4].

Thus, the results of the investigation performed allows us to assume that the seismic gap, by analogy with the acoustic gap, which is observed at fracture of metallic specimen, is connected with the fracture localization in the earth crust, decrease of the fracture process zone, formation of the main fault and its further stable development.

The described changes in the metallic specimen occur in transition from the stage III of damage accumulation to the next stage IV (Fig. 9). It is known that such a transition is accompanied by the acceleration of the damage development before the fracture and is described by the power relations of L.V. Kachanov for the case of static loading or P.C. Paris for the cyclic one.

As was shown in [2, 20], the Ω - function of the cumulative seismic deformation [21], and also S - function [5], which is the weight sum of basic seismic events can be used as the analog of the total damage of specimen at the analysis of seismic activity.

Since these functions include both the number of events and their energy, they, as it seems, most of all reflect the process of the gradual accumulation of damages before the main event, and they are equivalent (in physical sense) to the damage measure introduced by L.M. Kachanov and Yu. N. Rabotnov, that determines the total area of all damages and includes both the number and the length of defects.

The carried out analysis of the foreshock seismic activity before the earthquakes for three regions of the world [2, 20] with the use of the S - function confirms the regularities observed during the development of damages in the metallic specimens. So, it was shown that the higher the magnitude of future earthquake, the higher the average rate of the dissipation of cumulative seismic energy, which as assumed to be proportional to the cumulative length of the faults formed.

Data of the estimation of the rate of change in the S- parameter (dS/dt) as a function of S and the magnitude M of the forthcoming earthquake showed that the obtained kinetic diagrams are described in their middle part by the power relation, similar in form to the Paris equation, describing the rate of the fatigue crack growth:

$$dS/dt = A_1 (M\sqrt{S})^m ,$$

where m is the exponent that depends on a region; it was found to be close to the exponent in the Paris relation that varies from 2 to 4 for the majority of metallic materials. Similarly to the diagram of fatigue fracture, the kinetic diagrams of seismicity are characterized by the threshold value of the parameter $(M\sqrt{S})_{th}$.

A similar diagram of seismicity was plotted [2, 22] using data given in [21], in which the Ω-function was used to describe the acceleration of the seismic activity before the volcanic eruption. This diagram shows that the rate of seismic process is connected with the Ω- parameter by a power relation.

Thus, the kinetics of the processes, which occur in the earth crust and are connected to the preparation of earthquakes or volcanic eruptions, seems to be similar to the kinetics of damage accumulation in the metallic specimens before fracture.

Summary

Analysis of damage accumulation process in metallic specimens under different loading conditions with the use of mechanical and physical methods allows us to establish the following common criteria characterizing this process on different scales:

- correlation radius of microcrack accumulation process (R_y) and correlation radius of activation of acoustic or seismic events(R_C);
- number (N_C), length (L_C) and density (n) of microcracks (faults) in the fracture localized zone, fracture magnitude (M*);
- number (N_C) and magnitude (M) of acoustic (seismic) events;
- concentration criterion (k) of damage accumulation (microcracks, faults, acoustic or seismic events);
- exponents in power (b_C) and exponential (c) relations, describing cumulative distributions of number of microcracks (faults) on their length, number of acoustic emission signals (seismic events) on their magnitude (b_{AE}, b_S, c_{AE}, c_S) and number of fragments on their mass ($1/m_o$);
- time periods of acoustic (T_{AE}) or seismic (T_S) gap related to the formation of macrocrack (fault);
- total damage of specimen evaluated in using the relative fracture area (ω), cumulative energy of seismic events (S), cumulative seismic deformation (Ω);

- rate of damage accumulation ($d\omega/dt$), rate of increasing the cumulative energy of seismic events (dS/dt) and rate of change in cumulative seismic deformation ($d\Omega/dt$);
- fractal dimension of multiple fracture pattern (D_C), acoustic (D_{AE}) or seismic (D_S) events.

REFERENCES

[1] M.V. Gzovskij: *Bases of Tectonophysics*. (Moscow, Nauka. 1975).

[2] L.R. Botvina: *Fracture: kinetics, mechanisms, common regularities* (Moscow, Nauka. 2008).

[3] L.R.Botvina, and M.R.Tuytin Reports of RAN, 2007. V.417. N 3, p.385.

[4] L.R.Botvina, P.N.Shebalin, and I.B.Oparina., Doklady Physics, (Translated from Doklady Akademii Nauk of Russia). Vol. 46, (2001) p. 119.

[5] V.I. Keilis-Borok, and L. N. Malinovskaya. Jour. of Geophys. Res. Vol. 69. (1964). p. 3019.

[6] D. D. Bowman, G. Ouillon, C.G. Sammis et al.: J. Geophys. Res. Vol. 103, B10. (1998), p. 24359.

[7] P.N. Shebalin P.N. Technophysics. Vol. 424 (2006) p. 335.

[8] L.R.Botvina, I.M.Petrova, I.V.Gadolina et al. Industry Lab. (2008) (in press).

[9] L.R.Botvina and T.B.Petersen. Doklady Physics, (Translated from Doklady Akademii Nauk of Russia). Vol. 46, (2001) p. 56.

[10] C.N.Scholz. *The mechanics of earthquakes and faulting*. (Cambridge Univ. Press, Cambridge, 2002).

[11] M. Golombek M., and D. Rapp. J.of Geophys. Research, Vol.102, No. E2 (1997) p. 4117.

[12] C. Joussineau and A.Aydin. J.of Geophys. Res. Vol.112 (2007), p. B12401.

[13] I.M. Rotwain, V.I. Keilis-Borok, and L.R. Botvina Physics of the Earth and Planetary Interiors Vol. 101, (1997), p. 61.

[14] L.R. Botvina., M.R Tyutin and N.A Zharkova, in "Deformation and fracture of materials". Proc. of Conf. Moscow: IMET RAS.(2006).

[15] S.N. Zhurkov, V.S.Kuksenko and A.I. Sluzker: Physics of solid. Vol. 11 (1969), p. 296.

[16] T. Hirata J. Geophys. Res. Vol. 94 (1989) p. 7507.

[17] A.O. Önsel, I. Main, O. Alptekin, P. Cowie. Tectonophysics. Vol. 257 (1996) p. 189.

[18] V.I.Keilis-Borok and I.M.Rotwain. Physics of the Earth and Planetary Interiors. Vol. 61. (1990), p. 57.

[19] H. Kanamori. In: Prediction: An Intern. Review (eds. D.W.Simpson and P.G.Richards), Maurice Ewing Ser. V.4, AGU, Wash. (D.C.) 1981. P.1-19.

[20] L.R. Botvina. Intern. Jour. of Fracture. Vol.128 (2004), p. 133.

[21] B. Voight B. Nature. Vol. 332 (1988) p. 125.

[22] L.R.Botvina, and I.B.Oparina. Intern. Jour. Fracture. Vol 106 (2000) p.33.